

June 2021

Performance Assessment of GNSS Augmentation System Using Quasi-Zenith Satellite System for Real-time Precise Positioning Method in Indonesia

Irwan Gumilar

Geodesy Research Group, Institut Teknologi Bandung, igumilar@gd.itb.ac.id

Brian Bramanto

Geodesy Research Group, Institut Teknologi Bandung, bramanto@gd.itb.ac.id

Rifky Yusuf Ananta

Geodesy Research Group, Institut Teknologi Bandung

Dwi Haryanto

Agency for the Assessment and Application of Technology (BPPT)

Hasanuddin Zaenal Abidin

Geodesy Research Group, Institut Teknologi Bandung, hzabidin@gd.itb.ac.id

See next page for additional authors

Follow this and additional works at: <https://dc.uwm.edu/ijger>



Part of the [Civil and Environmental Engineering Commons](#), and the [Earth Sciences Commons](#)

Recommended Citation

Gumilar, Irwan; Bramanto, Brian; Ananta, Rifky Yusuf; Haryanto, Dwi; Abidin, Hasanuddin Zaenal; Surono, Surono; and Kishimoto, Nobuhiro (2021) "Performance Assessment of GNSS Augmentation System Using Quasi-Zenith Satellite System for Real-time Precise Positioning Method in Indonesia," *International Journal of Geospatial and Environmental Research*: Vol. 8 : No. 2 , Article 4.

Available at: <https://dc.uwm.edu/ijger/vol8/iss2/4>

This Research Article is brought to you for free and open access by UWM Digital Commons. It has been accepted for inclusion in International Journal of Geospatial and Environmental Research by an authorized administrator of UWM Digital Commons. For more information, please contact scholarlycommunicationteam-group@uwm.edu.

Performance Assessment of GNSS Augmentation System Using Quasi-Zenith Satellite System for Real-time Precise Positioning Method in Indonesia

Abstract

The Quasi-Zenith Satellite System (QZSS) is one of the GNSS technologies owned by the Japanese government, which orbits around East Asia, Asia Pacific, and Oceania. One of the advantages of the QZSS satellite is that it corrects the measurements using precise ephemeris, clock, and other augmenting corrections, and is primarily used for the Real-Time Precise Point Positioning (RTPPP) method. This study aimed to examine the QZSS system's performance for RTPPP measurements in Indonesia. Magellan System Japan's (MSJ) receiver was applied to collect the GNSS and the augmenting data to perform the RTPPP. RTPPP method was then made into the static and kinematic scheme. Various methods were also carried out on each method, such as static, Real-Time Kinematic (RTK), and other RTPPP providers. The result is that the precision level of the RTPPP method for the static scheme using the QZSS augmentation could give precision up to 5 cm in the open sky condition. Similar to other RTPPP correction providers, QZSS-RTPPP took approximately 20 minutes for the initiation process. The Accuracy of QZSS-RTPPP reached approximately 20 cm caused by the epoch reference for the actual coordinate was in epoch 2012.0, while the RT-PPP observations were occupied in 2019. The precision and accuracy level of QZSS-RTPPP tend to be more unstable in light and heavy obstructed conditions. In the measurements against 20 benchmarks at ITB Jatinangor, the accuracy value for the QZSS-RTPPP ranged from 5-40 cm. The RTPPP QZSS method's average accuracy for the easting, northing, and height components, respectively, was 0.110 m, 0.056 m, and 0.120 m. Utilizing the QZSS RTPPP measurements at sea for the moving platform, the obtained horizontal component precision level was between 10 and 20 cm. On the other hand, the overall precision for QZSS RTPPP measurement over the land region for the moving platform was lower than one meter for horizontal components, while the vertical component was lower than two meters.

Keywords

QZSS, GNSS, positioning accuracy, static, kinematic, obstruction

Acknowledgements

Our gratitude goes to Pak Surono and Pak Wono from MSJ representatives in Indonesia who have provided the opportunity to use their receiver. We also thank PT. Geotronix Indonesia, which has provided the test data to us. We thank the reviewers for constructing suggestions on the manuscript. Lastly, thanks to students of the Geodesy and Geomatics Engineering Study Program ITB, who helped a lot in field measurements.

Authors

Irwan Gumilar, Brian Bramanto, Rifky Yusuf Ananta, Dwi Haryanto, Hasanuddin Zaenal Abidin, Surono Surono, and Nobuhiro Kishimoto

1 INTRODUCTION

The satellite-based positioning and navigation, or the so-called, Global Navigation Satellite System (GNSS), refers to a system consisting of more than one constellation that allows users to obtain three-dimensional position and time information (Hofmann-Wellenhof et al. 2007). Nowadays, we can observe six GNSS constellations that operate globally and regionally due to the rapid development of the GNSS technology by several countries. The Global Positioning System (GPS)/America, Glonass/Russia, Galileo/Europe, and Beidou/China are the four GNSS constellations globally operating. Meanwhile, the regional satellites that are in operation are Japan's satellite-based positioning system, the Quasi-Zenith Satellite System (QZSS), and the Indian Regional Navigation Satellite System (IRNSS) that developed by India (Teunissen and Montenbruck 2017). All of the mentioned GNSS systems can be observed in Indonesia, except for the IRNSS, which can only be optimally observed at the western part of Indonesia based on the IRNSS extended coverage area (Thombre et al. 2016). The absolute and differential GNSS positioning method can take advantage of the existence of these systems. For example, the accuracy is improved in various environments and conditions when utilizing the Beidou satellite for the static and Real-Time Kinematic (RTK) GNSS methods (Gumilar et al. 2018; Bramanto et al. 2017; Gumilar et al. 2017).

The Japanese QZSS, aside from the Beidou satellite, is another satellite that operates in the Asia Pacific region, including Indonesia. Michibiki was the first QZSS satellite launched on September 11, 2011, and fully operated in 2013. In 2017, two quasi-zenith orbit (QZO) satellites and one geostationary orbit (GEO) satellite were launched in the year 2017 (JAXA 2017). These satellites are forming an "8" orbit shape (for the QZO's satellites) that covers Japan, East Asia, and the Oceania region (Murai 2014), as seen in Figure 1. Utilizing this orbit, the high elevation angle (with elevation close to 90°) assures its compatibility with GPS satellites in the Japan region. The QZSS satellites are intended to be used in urban areas with obstructions in the form of buildings and mountainous topographic areas (Teunissen and Montenbruck 2017).

The QZSS augmentation on GPS generally improves the satellite-based positioning performance. Krasuski (2015) reported that the GPS/QZSS solution improves the accuracy by 0.398 m, 0.432 m, and 0.285 m for the X-axis, Y-axis, and Z-axis in the Single Point Positioning (SPP) method, respectively. Improvements also apply to the static differential method when utilizing the GPS/QZSS satellites. Such combination increased the probability of phase ambiguity resolution, improved the satellite geometry or known as dilution of precision (DOP), and increased the satellite visibility (Wu et al. 2004; Zhang et al. 2007; Takahashi 2004). When using the QZSS satellite for the RTK and Precise Point Positioning (PPP) method, the utilization of the QZSS satellite also improved the positioning accuracy and ambiguity fixing ratio in the Asia-Pacific region (Zhu et al. 2020; Takasu et al. 2009).

In Indonesia, very limited studies of QZSS augmentation on satellite-based positioning have been conducted, particularly for the observation made by the so-called Real-Time Precise Point Positioning (RTPPP) method. A previous study from Gumilar et al (2021) showed that the accuracy of the QZSS augmentation for the RTPPP method was estimated to be less than 12 cm. However, it was only evaluated on a static platform. Nevertheless, the previous study of QZSS in Indonesia indicates that QZSS can

be used for many various activities in Indonesia. This study explores the performance and utilization of the QZSS augmentation system for the RTPPP method. This study is not only limited to a static platform but also a kinematic platform. Valuable suggestions for future development and positioning applications are expected from this study, particularly for Indonesia.

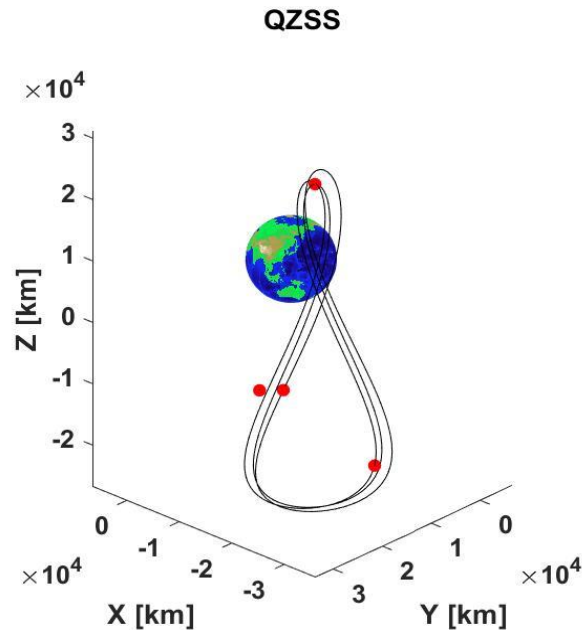


Figure 1. The trajectory (black lines) of QZSS orbit. Red dots represent the QZSS satellite at the same time.

2 THE GENERAL CONCEPT OF RTPPP

Prior to the existence of the RTPPP method, we mainly used the Precise Point Positioning (PPP) to obtain high accuracy level of less than a few centimeters by using a single GNSS receiver (El-Hattab 2014; Moschas et al. 2014). The difference between the so-called PPP and RTPPP is how the GNSS data processing is made. In PPP, the precise orbital and clock should be downloaded from the corrections providers, such as the International GNSS Service (IGS). Since both highly accurate orbital and clock are transmitted to the user using augmentation satellites, the user's position can be made in real-time.

Several error sources presented in the data need to be taken into consideration. First, the ionospheric-free linear combination (IF) is applied to remove the first-order ionospheric delays (Kouba and Héroux 2001). The mathematical expression of IF code and carrier-phase measurement is shown in Equation (1).

$$\begin{aligned}
 P_{IF} &= \frac{f_1^2}{(f_1^2 - f_2^2)} P_1 - \frac{f_2^2}{(f_1^2 - f_2^2)} P_2 \\
 \Phi_{IF} &= \frac{f_1^2}{(f_1^2 - f_2^2)} \Phi_1 - \frac{f_2^2}{(f_1^2 - f_2^2)} \Phi_2
 \end{aligned} \tag{1}$$

Further, Equation (1) can be defined as:

$$\begin{aligned}
 P_{IF} &= \rho + T + c(\delta t_r - \delta t^s) + (b_{r,IF} - b_{IF}^s) + \varepsilon_{IF} \\
 \Phi_{IF} &= \rho + T + N_{IF} + c(\delta t_r - \delta t^s) + (\varphi_{r,IF} - \varphi_{IF}^s) + \varepsilon_{IF}
 \end{aligned} \tag{2}$$

where P_{IF} and Φ_{IF} is the respective IF code and carrier-phase; f_1 and f_2 are the two frequencies of GNSS signal; P_i and Φ_i with $i = 1,2$ is the code and carrier-phase measurement, respectively. ρ is the geometric distance; T is the tropospheric delay; δt_r and δt^s are the receiver and satellite clock offset, while c is the speed of light in a vacuum condition; $b_{r,IF}$ and b_{IF}^s are the respective receiver and satellite hardware delay; $\varphi_{r,IF}$ and φ_{IF}^s are the uncalibrated phase delays (UPD; Ge et al. 2008); N_{IF} is the IF ambiguity of carrier-phase in length unit; the last term of ε_{IF} is the sum of noises.

In a general perspective, a least square adjustment is performed to retrieve expected information. Considering the satellite hardware delays also exist in the satellite clock products, and receiver hardware delay is presented in receiver clock and applying both precise orbits and clocks to Equation (2), the estimated parameters are the 3D coordinates, receiver clock, tropospheric delays, and ambiguities.

3 QZSS OVERVIEW

In general, the QZSS system consists of two main segments, i.e., space and control segment. The QZO and GEO satellites are the constituent of the space segment that operates in a highly inclined elliptical orbit (HEO) satellite. The control segment consists of three ground-based control stations. They are the monitoring stations (MS), master control stations (MCS), and tracking control stations (TCS) that have different purposes. The QZSS and other GNSS satellite signals are monitored by the MS spread across Japan, East Asia, and Oceania. MCS handles the observation signal data transferring from the MS. Later in the MCS, both orbital and time parameters will be estimated and tackle any outliers present in the GNSS signals. The corresponding parameters are then transferred to the TCS and upload to the QZSS satellites. In addition, TCS also communicates with the QZSS satellites. Furthermore, QZSS satellites broadcast a ranging signal in the frequency bands L1, L2, L5, L6, and S, which is compatible with GPS signals and can be used in conjunction with them (CO 2018). Further detail on these signals can be seen in Table 1.

The precise orbit and clock corrections of MADOC (Multi-GNSS Advanced Demonstration Tool for Orbit and Clock Analysis) and CLAS (Centimeter Level Augmentation Service) are transmitted through the L6 band frequency. These signals transmit the necessary GNSS products used in the RTPPP method, such as orbit and clock correction on a regular basis. MADOC products are referenced to the IGS final

orbits and clock corrections (El-Mowafy 2018). MADOCA service is regionally available. Meanwhile, CLAS is designed to be used only in Japan (Namie and Kubo 2021). Also, PS-QZSS reported that the desired centimeter-level accuracy is obtained in less than a minute for CLAS. On the other hand, MADOCA needs approximately 20 to 40 minutes to achieve the desired centimeter-level accuracy (Namie and Kubo 2021).

Table 1. Signal used in QZSS.

Center Frequency (Mhz)	Signal	Service
L1 (1575.42)	L1C/A	Satellite Positioning Service
	L1C	Satellite Positioning Service
	L1S	Sub-meter Level Augmentation Service (SLAS) Satellite Report for disaster management
	L1Sb	Satellite Based Augmentation System (SBAS)
L2 (1227.60)	L2C	Satellite Positioning Service
L5 (1176.45)	L5	Satellite Positioning Service
	L5S	Experimental service
L6 (1278.75)	L6	L6D Centimeter Level Augmentation Service (CLAS) L6E Multi-GNSS Advanced Demonstration Tool for Orbit and Clock Analysis (MADOCA)
S (2000.00)	S	QZSS Safety confirmation service

4 THE EXPERIMENTAL SETUP

This study used both MSJ's GNSS receiver of Albicila version or Luschnia 2+ version (Figure 2) to assess the augmentation positioning performance. We evaluated the QZSS positioning performance in both static and moving platforms. The QZSS augmentation positioning coordinates were compared with the static method, Real-Time Kinematic (RTK) method, and other augmenting service providers, such as Differential GPS (DGPS) from Veripos, Real-Time Extended (RTX) from Trimble, and ATLAS augmenting satellite from Hemisphere (ATLAS-RTPPP).

The data acquisitions have been taken in several places in Indonesia, i.e., West Java Province, Central Java Province, and the Indian Ocean. The dual-frequency geodetic-type GNSS receivers were used for the static method and obtained 'true' coordinates for validation. This is done for cases when a comparative assessment can be done. Furthermore, we used a final precise ephemeris and clock in the data processing. ITB1 was considered a stable reference point. It lies over the roof and is continuously maintained by the Geodesy Research Group of Institut Teknologi Bandung. Based on multi-years of observations data, the derived positions were varying within millimeters precision. Hence, it was used as a reference point in this study.

Several schemes were made in this study. First, we evaluated the effect of environmental obstruction in QZSS augmenting positioning. Next, setting up three different obstruction conditions as follows: open sky where there is no obstruction in the antenna's line of sight; slightly obstructed; and highly obstructed condition (Figure 3). The observations were taken for several hours at Institut Teknologi Bandung (ITB) using the Albicila version of MSJ's receiver and compared with ATLAS-RTPPP and static

methods. By comparing it to the static method, both the accuracy and precision of the QZSS augmenting system can also be evaluated.



Figure 2. Albicila Version (upper) and Luscinia 2+ Version (lower) of MSJ's receivers used in this study.

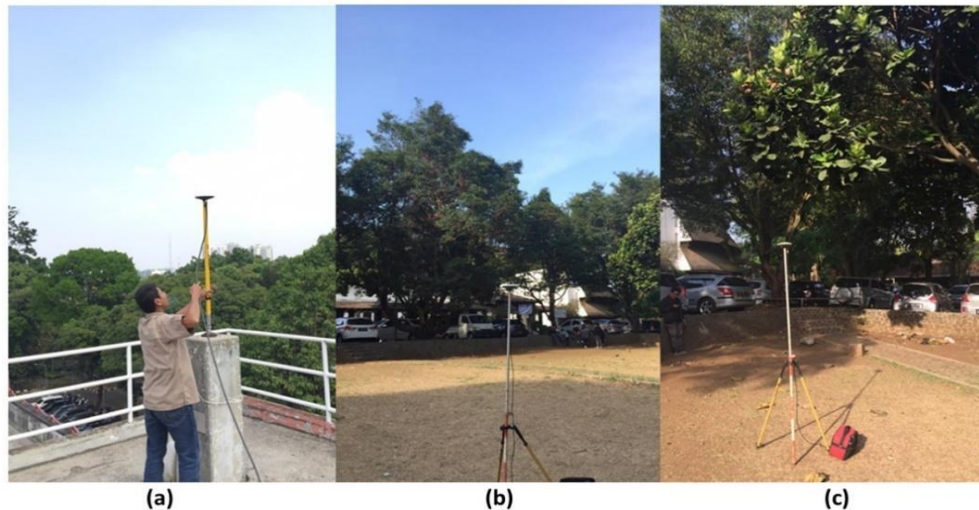


Figure 3. The measurement of RTPPP for the (a) open sky, (b) slightly obstructed, and (c) heavily obstructed conditions.

In addition, we also performed a similar scheme using the Luscinia 2+ version of MSJ's receiver in Banyumas, Central Java, Indonesia. The observations in Banyumas were taken for a day. Luscinia 2+ is a recent version of MSJ's receiver that can also observe and track the QZSS positioning and augmenting section. Hence, we could examine whether the changes in receiver hardware will affect the positioning performance. In this scheme, QZSS augmenting-based positions were only compared with the static method.

Moreover, we split the antenna's output into two separate receivers. The first receiver used an MSJ receiver, while a Veripos receiver was used for the second receiver. Different satellite-based positioning methods were used for each receiver. For example, the RTPPP method was implemented in the MSJ receiver, and the DGPS method was used in the Veripos receiver. It should be noted that the Veripos receiver only observed GPS signals, while the MSJ receiver observed both GPS and QZSS signals. Figure 4 shows the receivers and antenna used in this study. In this scheme, the observations were made by PT Geotronix Indonesia. The observation lasted for about three days for the QZSS-RTPPP method and two days for the DGPS-Veripos method.

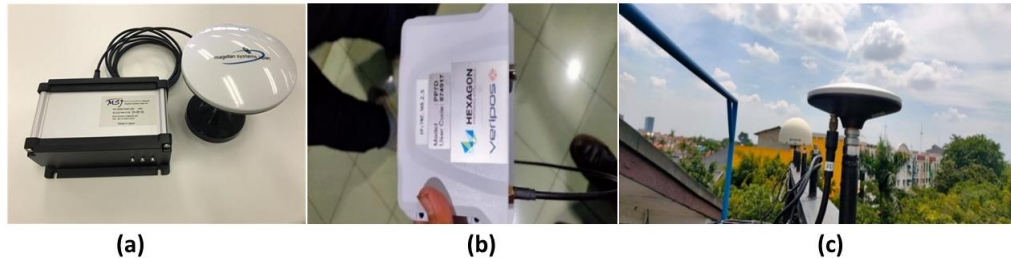


Figure 4. The instrument and setup used at PT Geotronix Indonesia. From left to right are the MSJ receiver (a), Veripos receiver (b), and antenna (c), respectively.

We also measured 20 benchmark points using the QZSS-RTPPP method at the ITB Jatiningor. Almost similar to the previous scheme, we conducted static, RTK, and ATLAS-RTPPP observations as a comparison. A static observation approach lasting around 30 minutes was performed, with a baseline length of approximately 500 m. The static method parameters used in this scheme were almost similar to previous measurements in ITB. The corresponding results were used as a valid coordinate for the validation. The nearby Continuously Operating Reference Stations (CORS) GNSS, namely CSUM maintained by the Geospatial Information Agency of Indonesia (BIG), was used for the RTK method. The baseline length between CSUM and rover was approximately 7 km. For the RTPPP method, the observations were made in a one second interval for approximately slightly more than 30 minutes long. The first 20 to 30 minutes was intended to perform the initialization process required for the RTPPP (both QZSS-RTPPP and ATLAS-RTPPP) method. The last five minutes of RTPPP observations were used for the analysis.

Lastly, we utilized the QZSS RTPPP positioning in a moving platform on Indonesia's sea and land areas. This scheme aimed to evaluate the precision level when utilizing the QZSS-RTPPP in a moving platform. The measurement for the kinematic method used the Albicila version of MSJ's receiver. In some cases, other RTPPP methods were also used as a comparison. The measurements on the land were taken in Padaleunyi Toll-road, Bandung, while the measurements on the sea were carried out at the Kepulauan Seribu and around the island of Sumatra. The measurements in the Java Sea involved the RTPPP-ATLAS method and the Veripos DGPS method and took approximately three hours of observation. The measurements around the island of Sumatra were carried out for a month on the Baruna Jaya Ship, which belongs to the Agency for the Assessment and Application of Technology (BPPT). The ship trajectory is displayed in Figure 6. Figure 7 shows the summary of the data acquisitions strategy.

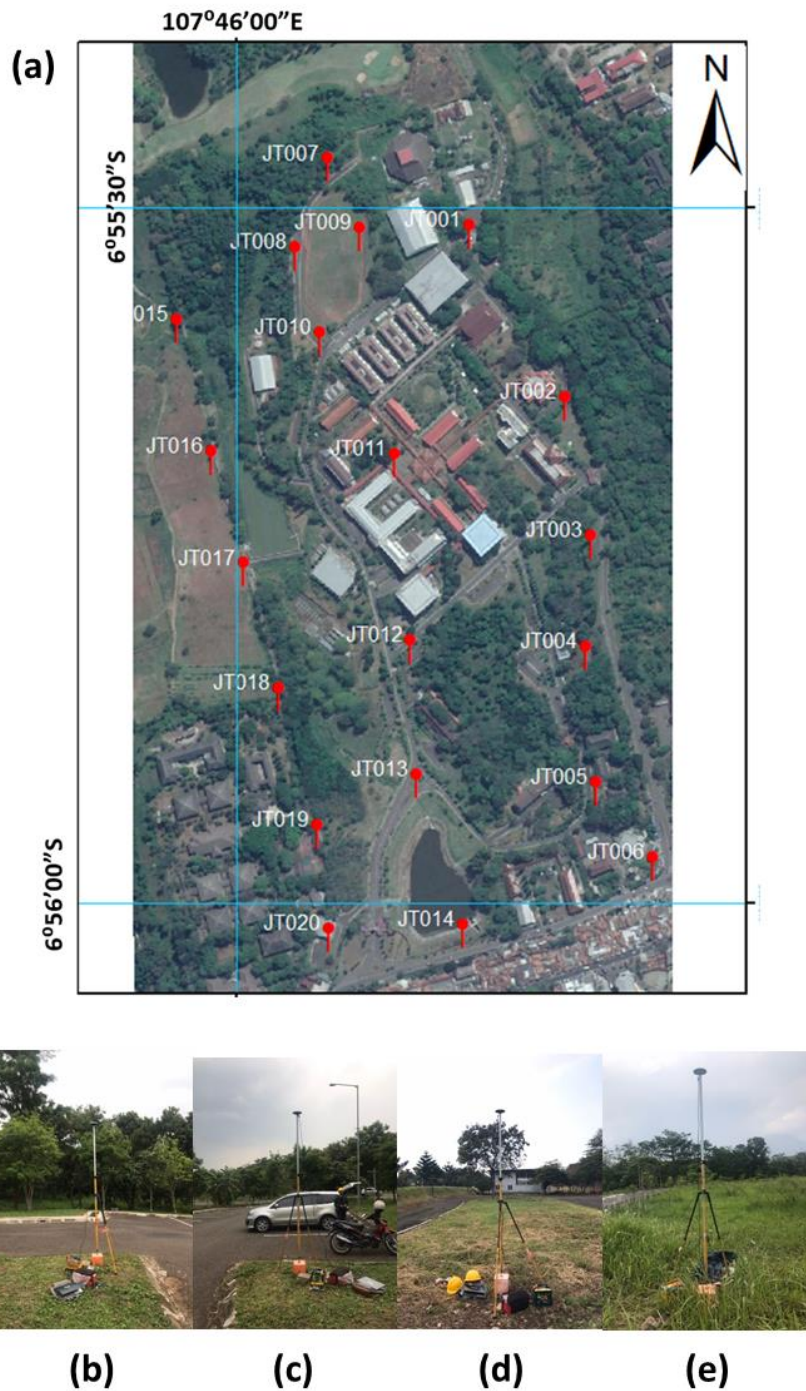


Figure 5. The distribution of observation points at ITB Jatinangor (a) and the field measurement documentation at points J001 (b), J006 (c), J010 (d), and J018 (e).

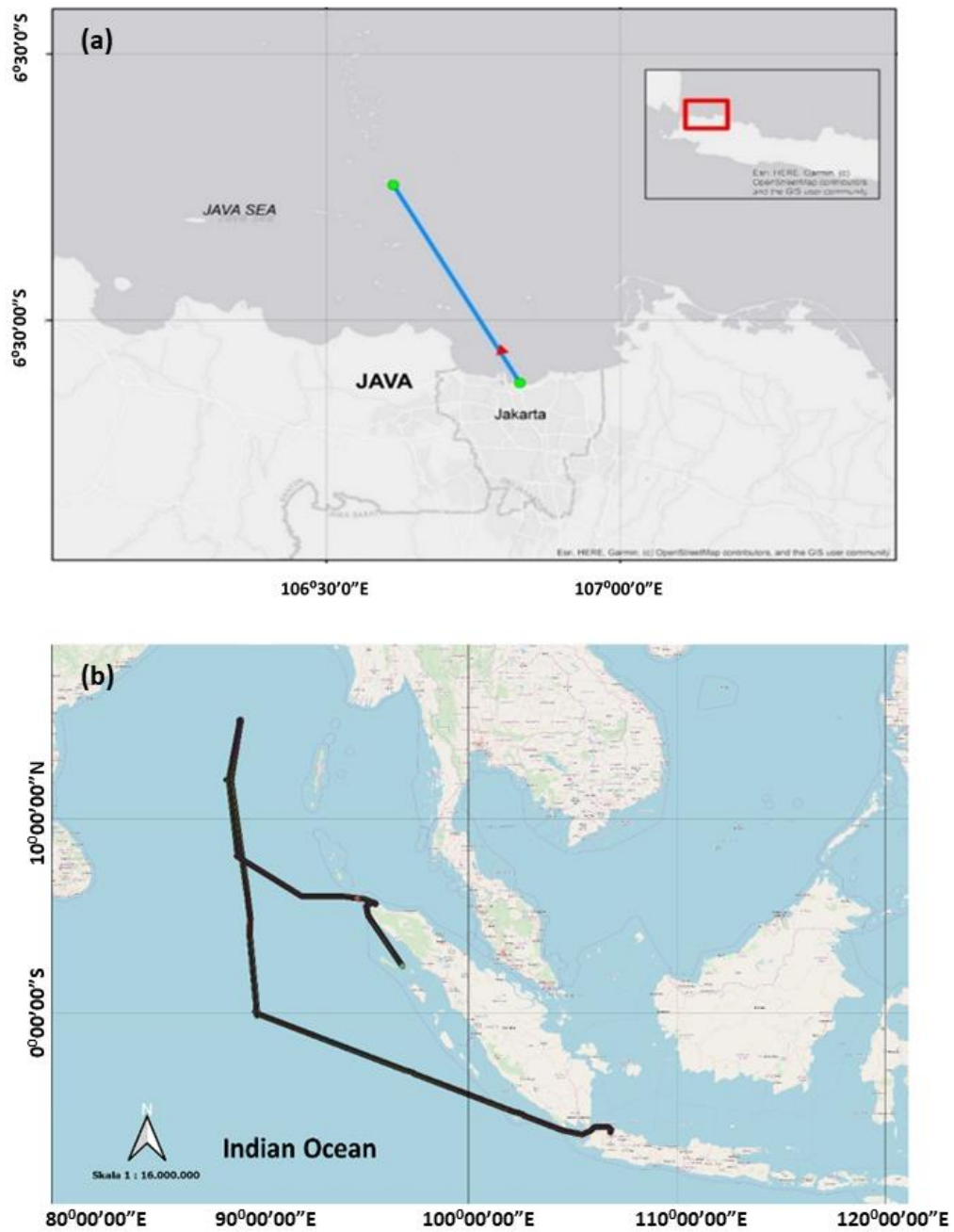


Figure 6. Ship trajectory at Kepulauan Seribu (a) and Sumatra Island (b).

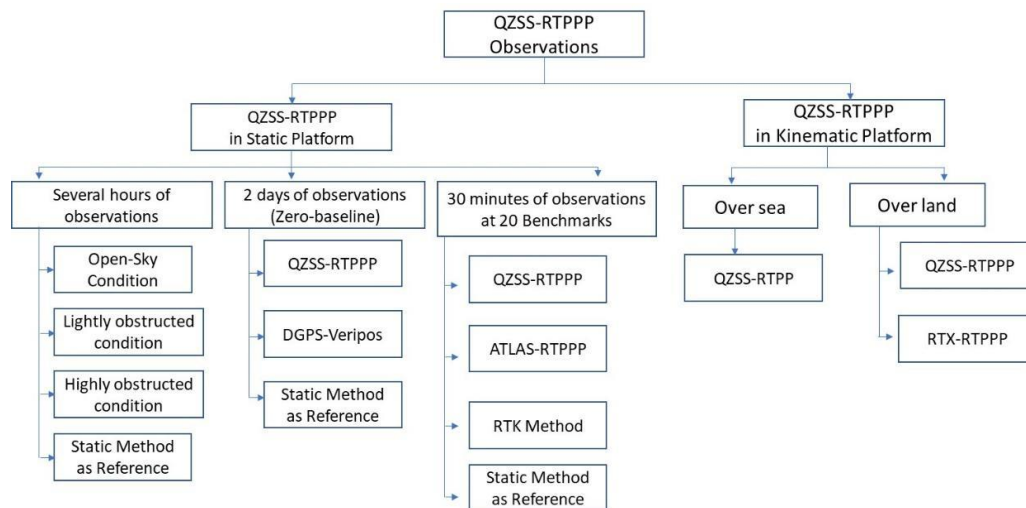


Figure 7. Data acquisition strategy used in this study.

5 RESULTS AND DISCUSSION

The results of the first at ITB were the level of precision, the accuracy of the QZSS RTPPP, and its comparison with other RTPPP correction providers. In determining the accuracy value, the RTPPP method's results are compared with the results of the short static method with a relatively short baseline between the base station and rover. The static method's reference point refers to the 2013 Indonesian Geospatial Reference System Datum (SRGI 2013). SRGI 2013 refers to ITRF 2008 epoch 2012. This information is essential for the further analysis of the level of accuracy.

The level of precision for horizontal and vertical components for open sky, slightly obstructed, and heavily constructed conditions, which can be viewed in Figure 8. Figure 8a shows the horizontal and vertical QZSS-RTPPP Root Mean Square (RMS) for open-sky condition ranging below 10 cm (after initialization). However, the RMS QZSS-RTPPP is still lower than the RTPPP-ATLAS's. RTPPP-ATLAS also appeared to be more stable than QZSS-RTPPP throughout the observation. The initialization process of both methods took 15-30 minutes. Furthermore, the horizontal and vertical RMS of QZSS-RTPPP ranged from 20-30 cm and more prominent than the RMS of RTPPP-ATLAS (smaller than 10 cm) on measurements with slight obstruction, as seen in Figure 8b. The previous studies also corroborate and give a similar initialization time and results (Ramachandran et al. 2019; Alcay and Turgut 2017; Bramanto et al. 2015). At the heavily obstructed condition (Figure 8c), the horizontal and vertical RMS QZSS-RTPPP is within the meter level, while the RTPPP-ATLAS is still in the centimeter range. These results indicated that the level of precision of the QZSS-RTPPP is adequately affected by obstruction around the observation point (Ramachandran et al. 2019).

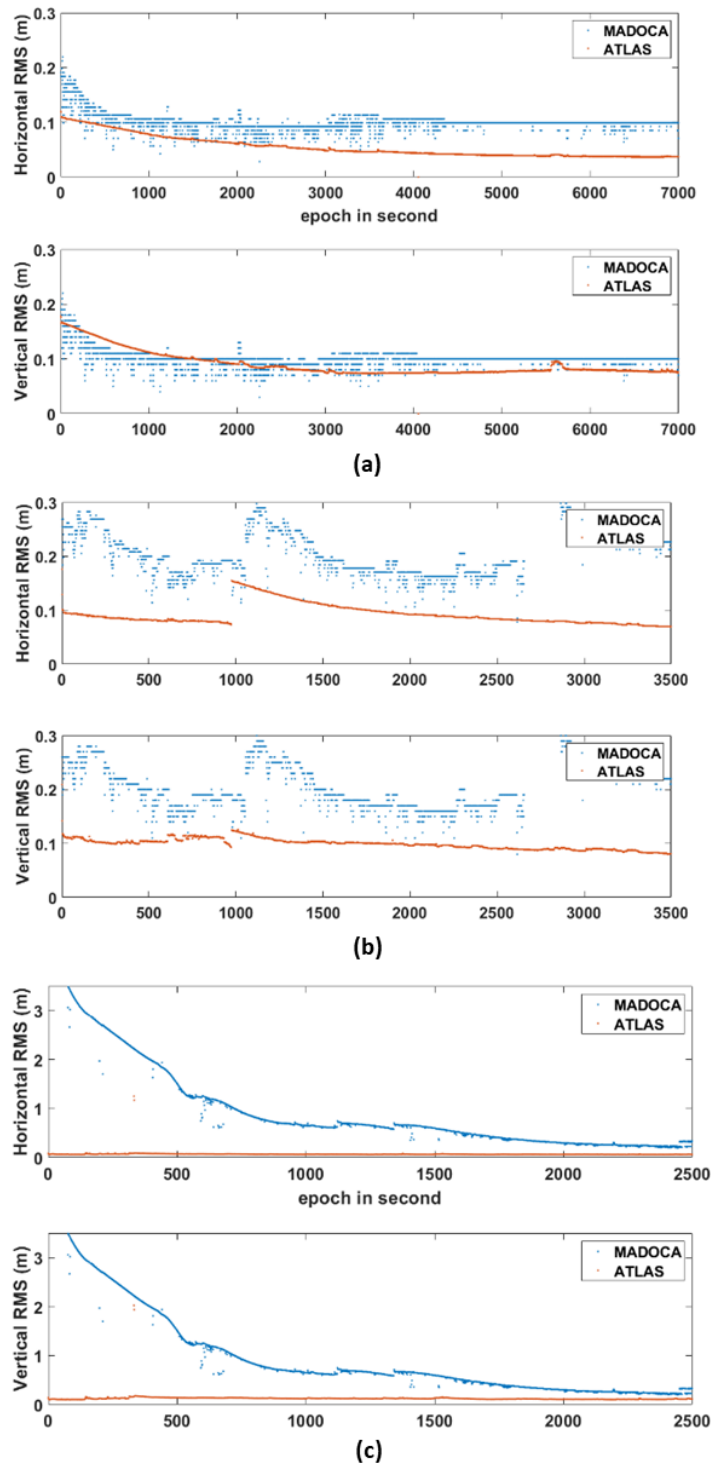


Figure 8. Precision level for the (a) open sky, (b) slightly obstructed, and (c) heavily obstructed condition at ITB. The Horizontal axis indicates epoch in the second unit.

Each position component's value is subtracted with the referenced coordinate (estimated from the static method) to assess the positioning accuracy, as shown in Figure 9. In an open-sky condition, the horizontal component's accuracy for each method is approximately 20 cm (based on the average coordinate). This difference is due to the epoch difference in the epoch reference that is used. The epoch reference for the actual coordinate is 2012.0 (BIG 2013), while the RTPPP observation was occupied in 2019. We expected the coordinate differences of approximately 21.79 cm to South-East direction, which align with the corresponding result. A significant difference for the vertical component occurs in the QZSS-RTPPP method, while the ATLAS-RTPPP tends to be better (within cm level). This difference is possibly caused by the antenna offset errors in the QZSS-RTPPP instrument setting. However, further analysis needs to be done. The worst accuracy performance of QZSS-RTPPP occurs during the heavily obstructed condition. The difference reaches ± 5 meters in the horizontal component. On the other hand, RTPPP-ATLAS can maintain the positioning accuracy within the decimeter level.

In the measurements using the MSJ Luciana 2+ receiver, the horizontal and vertical RMS results were better than the earliest version. Figure 10 shows the horizontal and vertical RMS for QZSS-RTPPP for more than 24 hours of observation. Both horizontal and vertical RMS tend to be stable in centimeter-level and eventually lower than five millimeters after two hours of observations. Two spikes are shown in the data due to electrical problems and causing a re-initialization process. The resulting accuracy using the Luciana 2+ MSJ receiver can be seen in Figure 11. As already mentioned in the previous discussion, the horizontal component's accuracy reached approximately 20 cm due to differences in the observation epoch. Meanwhile, the accuracy of the vertical axis was estimated to less than 10 cm.

Other results show the variation of the QZSS-RTPPP-derived and DGPS-Veripos-derived positions. Figure 12 shows the horizontal discrepancy of the QZSS-RTPPP and DGPS-Veripos, and they were estimated within 1-2 decimeters. The vertical discrepancy, however, failed to achieve a similar result when we compared it to the known height value. It differed by approximately 3.5 meters. We argue that this is due to a systematic error when processing the actual coordinate value, as both methods gave a similar result. The time-series figure also reveals other interesting findings. Both methods, the QZSS-RTPPP and DGPS-Veripos, had a sinusoidal pattern present on the time-series data. The observed geometry satellite was possibly causing this behavior. In addition, the QZSS-RTPPP method still had a lower precision level compared to the DGPS-Veripos method, as seen in Figure 12.

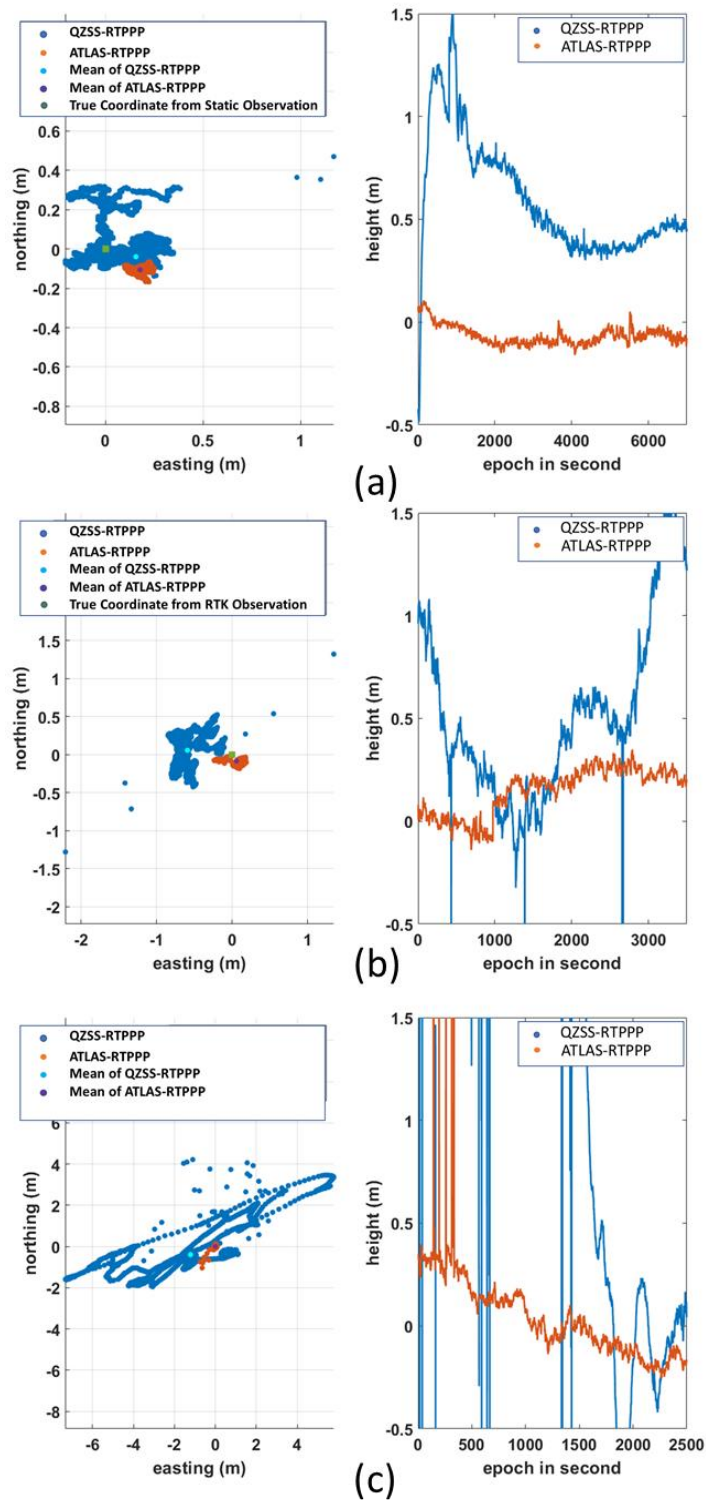


Figure 9. QZSS-RTPPP accuracy level for the (a) open Sky (a), slightly obstructed (b), and heavily obstructed (c) condition at ITB.

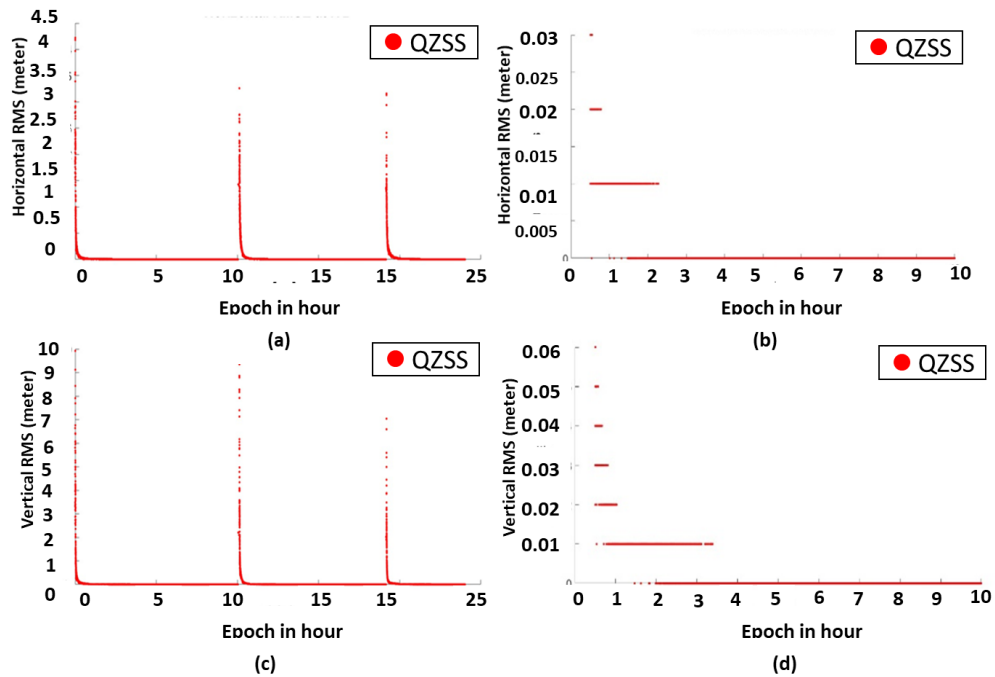


Figure 10. The precision Level of QZSS-RTPPP using the Lusciana 2+ version of MSJ receiver. The horizontal and vertical RMS are displayed in (a) and (c), respectively. (b) and (d) show the horizontal and vertical RMS during the first ten hours of observations.

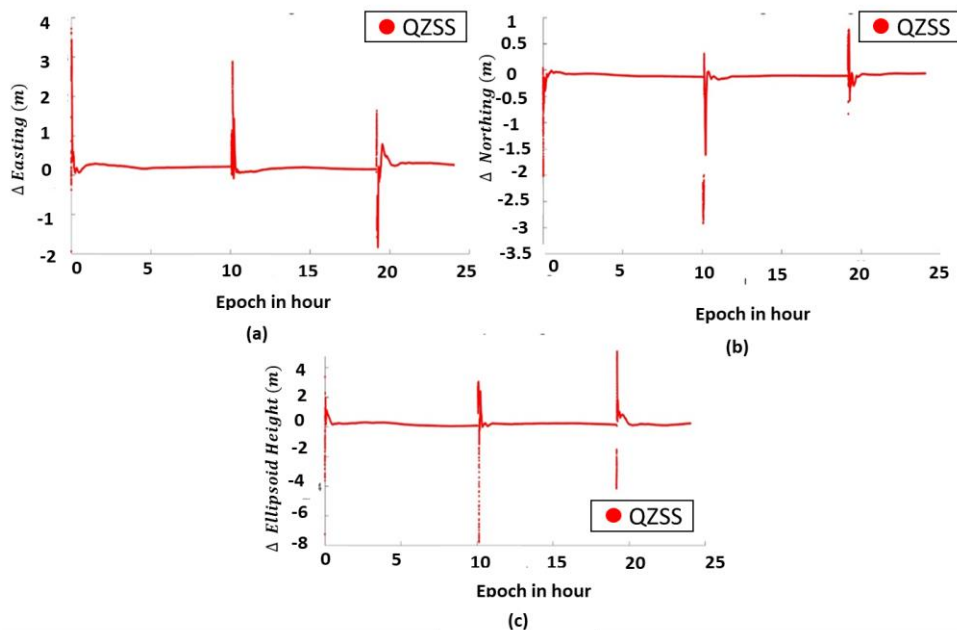


Figure 11. The difference of QZSS-RTPPP positions referring to the static's coordinates in (a) Easting, (b) Northing, and (c) up component.

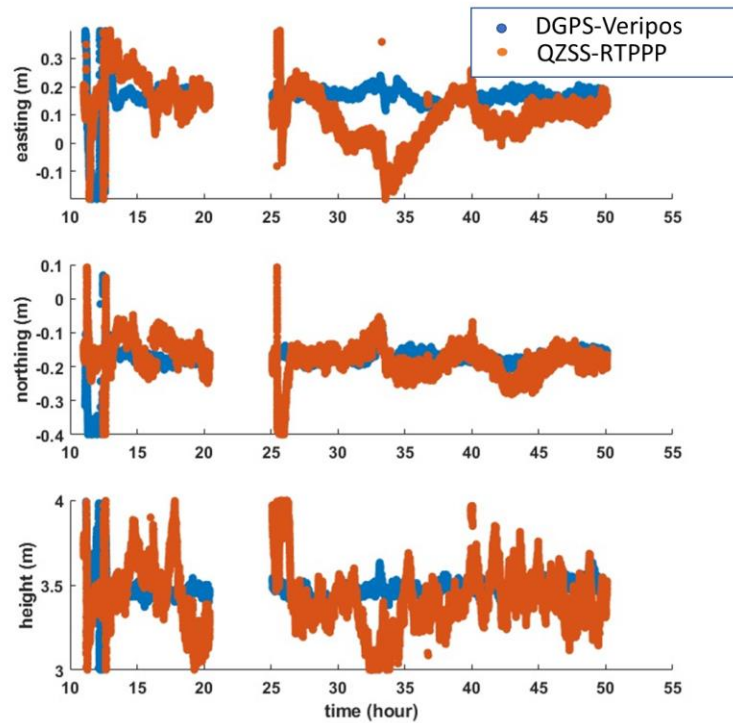


Figure 12. The time-series plot of QZSS-RTPPP and DGPS-Veripos for each component relative to their reference value.

At ITB Jatinangor, observations were performed over 20 benchmarks. The estimated coordinates using several methods (i.e., the QZSS-RTPPP, ATLAS-RTPPP, and RTK) were compared to the reference coordinates as estimated using the static method. Figure 13 shows both horizontal and vertical RMS for the QZSS-RTPPP method at JT001. After about 10 to 20 minutes, the RMS was obtained at the desired RMS level or its steady state (with less than 0.10 m and 0.20 m for the horizontal and vertical RMS, respectively). The observations that were made at other benchmarks also gave equivalent results. The ATLAS-RTPPP method's measurement goes through a similar procedure of initialization. However, the behavior of the initialization process cannot be shown since the positions were only recorded after achieving the desired RMS value. Furthermore, the RTK method's measurement has an RMS value of roughly 5 cm, which is better than the RMS of the QZSS-RTPPP and ATLAS-RTPPP method.

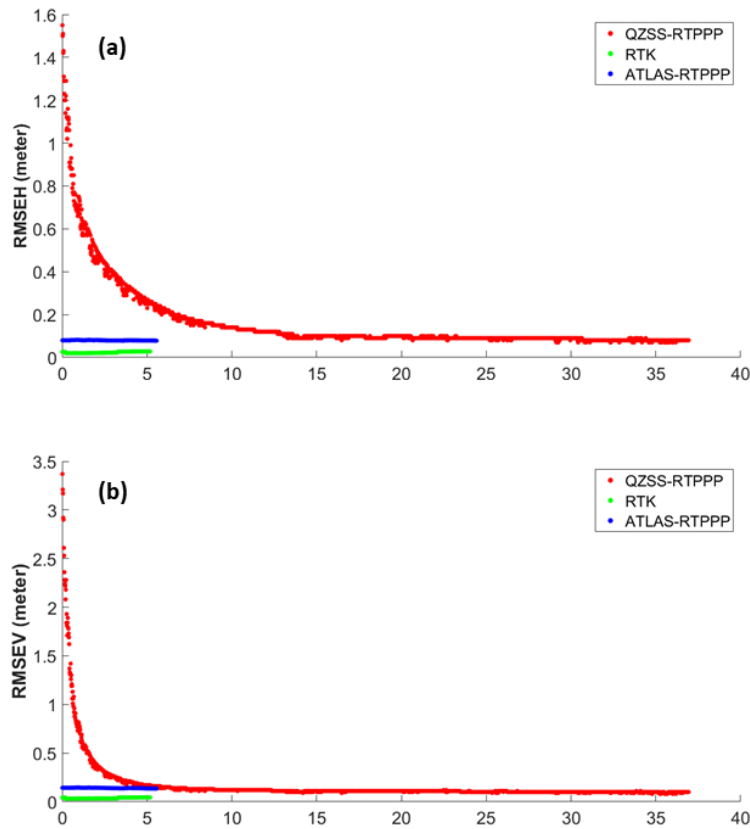


Figure 13. The time-series of the RMSE at JT001 using QZSS-RTPPP, ATLAS-RTPPP, and RTK approaches. The upper panel shows the horizontal RMSE, while the lower panel displays the vertical RMSE. The horizontal axis is in minute(s) unit.

The overall accuracy for each method (QZSS-RTPPP, ATLAS-RTPPP, and RTK) at ITB Jatinangor is then evaluated by comparing them to the static method positions as a reference coordinate. The horizontal position residue for each method is shown in Figure 14. The RTK method gives the best performance among others with an average position residue of lower than 5 cm. This also applies to the vertical component, where RTK gives the highest accuracy among others with an average discrepancy of less than 10 cm. The QZSS-RTPPP seems to have a better horizontal and vertical position residue than the ATLAS-RTPPP. It varies from 5 to 40 cm relative to the reference coordinates. The average horizontal accuracy for easting and northing components for the QZSS-RTPPP method is estimated to 0.110 m and 0.056 m, respectively. The average vertical accuracy also gives a similar value that is estimated to 0.120 m. The ATLAS-RTPPP has almost the same accuracy level compared to the QZSS-RTPPP. The three-dimensional position discrepancy ranges from 5 to 60 cm.

As mentioned in the previous section, measurements were made in both ocean and land areas for setups implemented in moving platforms. In the first case, the measurement occupied during the travel from Jakarta to the Kepulauan Seribu was carried out using the QZSS-RTPPP and RTX-RTPPP methods. The RMS for the horizontal and vertical components of both methods can be seen in Figure 15. The accuracy of the

horizontal RMS for both methods after the initialization process for 20-30 minutes was smaller than 10 cm. RMS of the RTX-RTPPP reaches up to 5 cm and tends to be more stable. RMS of the QZSS-RTPPP tends to increase at the end of its destination. The QZSS-RTPPP's vertical RMS reached 10 to 40 cm, and the RMS increased as the final destination was reached. Meanwhile, the vessel speed based on the QZSS-RTPPP data seems more stable than the RTX-RTPPP when analyzing each method's speed stability (derived from position) at Figure 16. Those spikes were shown due to the hardware failure during the operation.

Figure 17 shows the results of QZSS-RTPPP measurements around the island of Sumatra for a more extended period. The measurements were carried out from November 12 to December 6, 2019, with a route from Jakarta to Aceh through the South Sumatra Sea. The observations were made to examine the consistency of data results generated from the QZSS satellite during a long period (26 days) using the RTPPP method. Figure 18 shows a sample of observations during 1-5 December 2019, neglecting the strange signature (stable RMS value of more than 1 meter), the average horizontal and vertical RMS value reach up to 20 cm. The operation had a lot of electrical problems due to various activities carried out on the boat. The hardware faulty is considered the reason for the substantial RMS (meter level) in several periods since the receiver is being used for a more extended period.

The land areas' measurement was taken along the Padaleunyi Toll road by car and took approximately one hour. We used the MSJ Albicila version for the QZSS-RTPPP and Trimble NetR9 for the RTX-RTPPP. The MSJ measurement epoch is set every 1 second, while the Trimble measurement epoch is adjusted every 2 seconds. The measurements were taken round-trip and started from the ITB - Pasteur Toll Gate - Soreang Highway Gate - Buah Batu Highway Gate - ITB. This measurement examines the QZSS performance when the receiver is in motion (kinematic) in the land area and compared with other RTPPP correction providers.

Both horizontal and vertical RMS for the QZSS-RTPPP and RTX-RTPPP methods in the Padaleunyi Toll Road measurements can be viewed in Figure 18. The horizontal and vertical RMS values have a diverse pattern in both methods. The horizontal RMS and vertical RMS in the moving platform are ranging from centimeters (cm) to meters (m). Neglecting the re-initialization process, the Horizontal RMS value in the QZSS-RTPPP data reaches up to one meter, while for the ATLAS-RTPPP reaches up to 50 cm. On the other hand, the vertical RMS value in the QZSS-RTPPP data reaches up to two meters, while the ATLAS-RTPPP data reaches up to one meter. QZSS-RTPPP data measurements on the highway road have undergone many re-initialization processes due to the profound obstruction condition, such as highway gates, flyovers, campus entrance gates, and tree canopies.

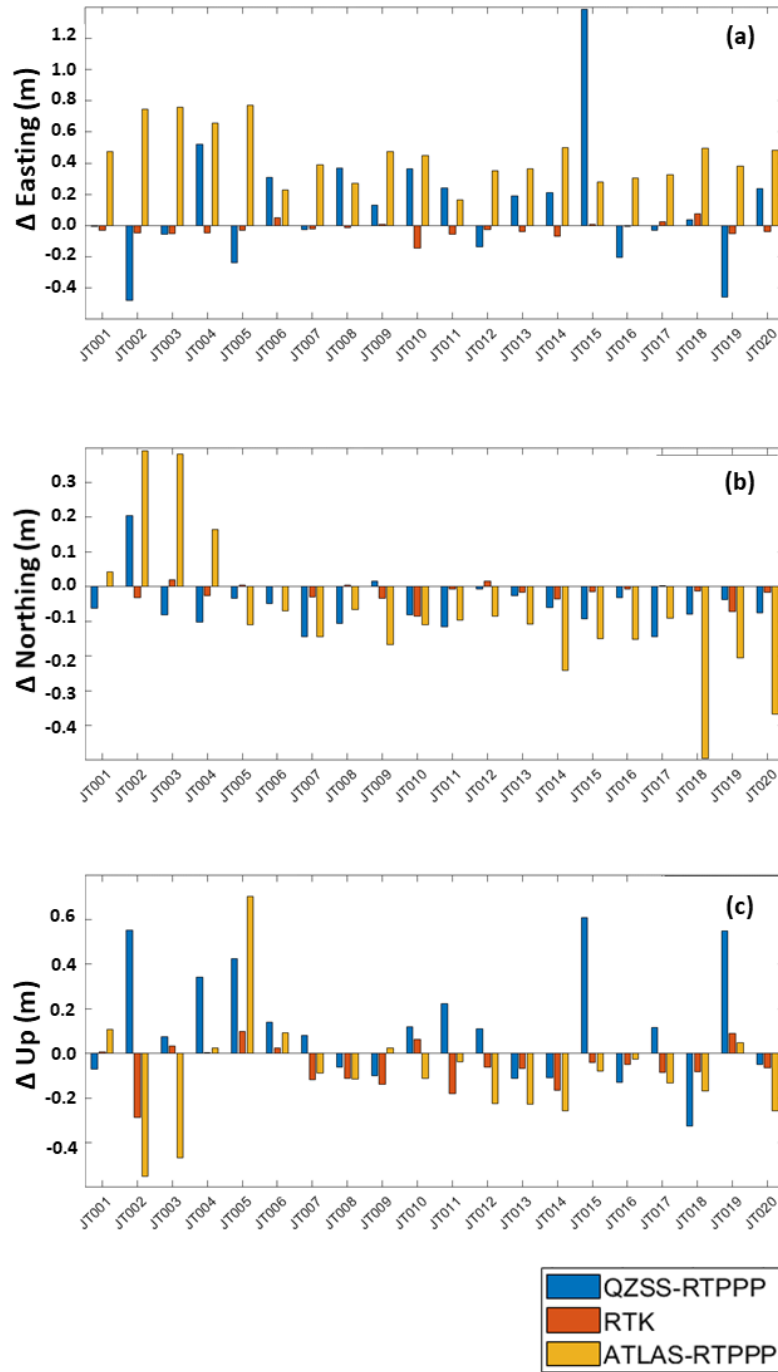


Figure 14. The overall accuracy of the QZSS-RTPPP, RTK, and ATLAS-RTPPP approaches at all ITB Jatinangor benchmarks. The upper, middle and lower panels display the easting, northing, and up components discrepancy relative to the static method.

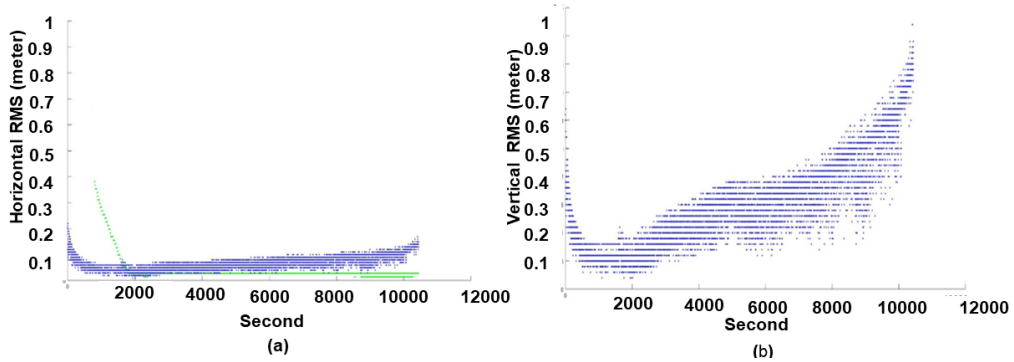


Figure 15. The precision of the QZSS-RTPPP (blue dots) and RTX-RTPPP (green dots) methods during the Jakarta-Kepulauan Seribu sail. The horizontal and vertical RMS is presented in (a) and (b), respectively.

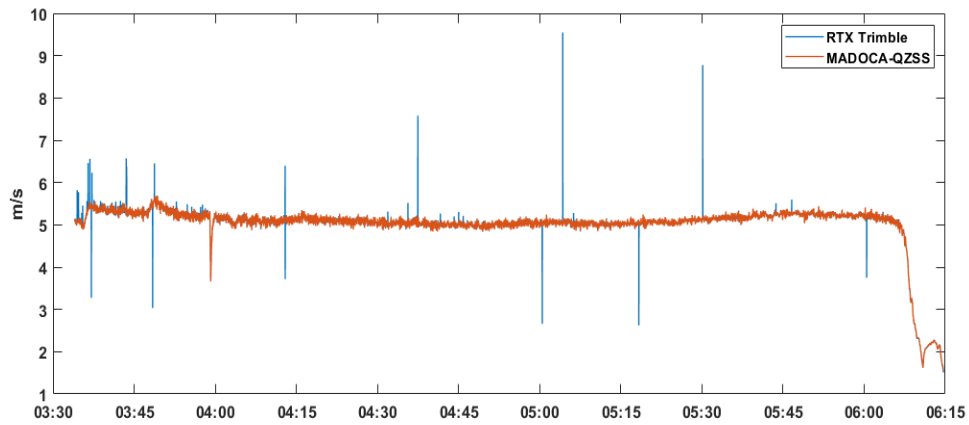


Figure 16. Vessel speed derived using QZSS-RTPPP and RTX-RTPPP method. Horizontal axis shows the local time (UTC+7).

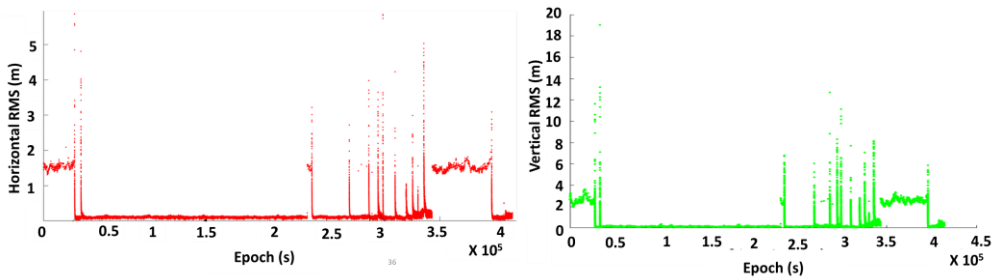


Figure 17. The horizontal (a) and vertical (b) precision level for the QZSS-RTPPP during the Sumatra sail.

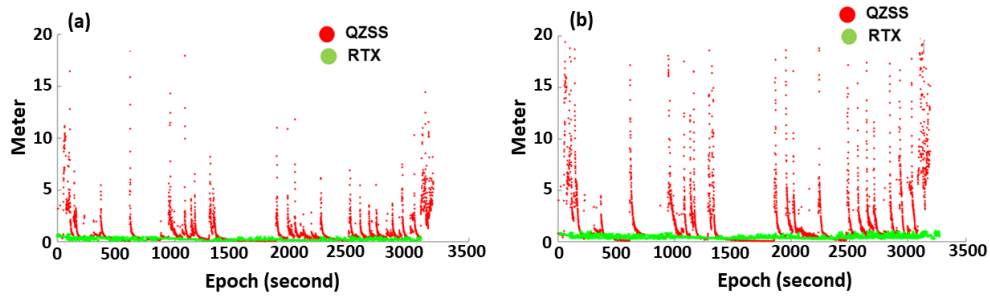


Figure 18. The horizontal (a) and vertical (b) precision level for the QZSS-RTPPP (red dots) and RTX-RTPPP (green dots) at the Padaleunyi Toll.

Figure 19 exhibits the estimated ellipsoid height from both QZSS-RTPPP and RTX-RTPPP at Padaleunyi Toll. The elevation is ranging from 660 to 820 meters over the ellipsoid. Visually, both indicate a similar result. However, taking a closer look at the time-series plot, it can be concluded that QZSS-RTPPP has a lot more considerable noise than the RTX-RTPPP (Figure 20). The RTX-RTPPP appears to be more stable in the obstructed environment.

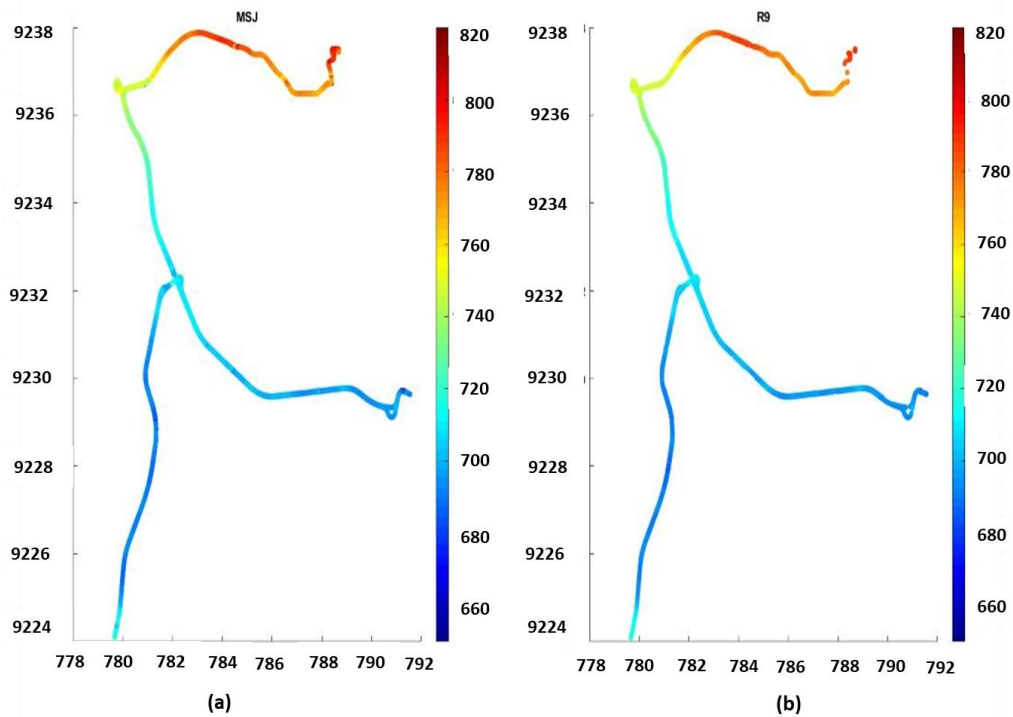


Figure 19. Estimated ellipsoid height from QZSS-RTPPP (a) and RTX-RTPPP (b) at the Padaleunyi toll. X-axis and y-axis are in kilometer units, while the color bar is in meter units.

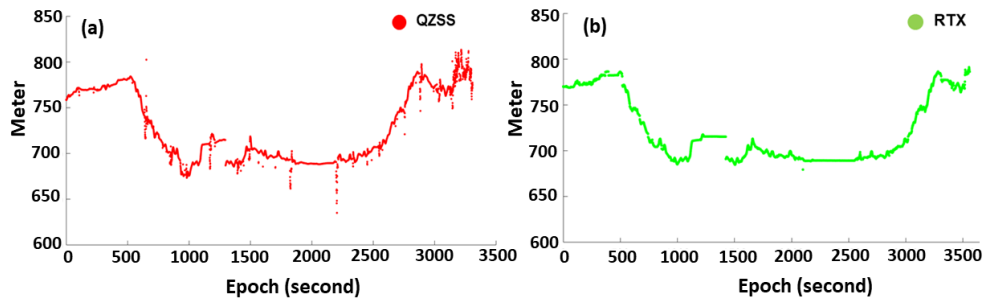


Figure 20. Estimated ellipsoid height from QZSS-RTPPP (a) and RTX-RTPPP (b) at the Padaleunyi toll over time.

6 FINAL REMARKS

This study reveals that the precision level of the QZSS augmentation on GNSS for the RTPPP approach is estimated up to 5 cm in an open-sky and static platform condition when using the MSJ receiver. However, to achieve such accuracy, we needed approximately 20 minutes for the initialization procedures. This also applies when we use other RTPPP correction providers (e.g., ATLAS-RTPPP). The accuracy of QZSS-RTPPP peaked at about 20 cm, caused by the different epoch references used for the static and RTPPP methods. In a slightly and heavily obstructed state, the precision and accuracy of QZSS-RTPPP tended to be more unstable than other RTPPP providers. The use of the QZSS-RTPPP method using the Luscinia 2+ version receiver showed a better precision level (less than 5 mm), while the accuracy level showed relatively similar results.

We can conclude from this study that the QZSS-RTPPP method has a sufficiently steady precision and mapping accuracy level based on the two-day comparison between QZSS-RTPPP and DGPS-Veripos measurements. However, both accuracy and precision were still lower than the DGPS-Veripos technique, indicating that more research is needed. The position discrepancy at 20 evaluation points (benchmarks) at ITB Jatinangor ranged from 5 to 40 cm for the QZSS-RTPPP. The easting, northing, and height components of the RTPPP QZSS technique have an average accuracy of 0.110, 0.056, and 0.120 meters. Although this value is still lower by few centimeters than the accuracy of the RTK approach, it is comparable to other RTPPP correction providers.

Overall horizontal and vertical RMS for QZSS-RTPPP was estimated to 20 cm and 40 cm in the moving platform over the sea areas, respectively. The relatively long GNSS campaign underwent multiple re-initialization processes due to the vessel's electricity and hardware instability. In a short measurement period, the QZSS-RTPPP tended to give a relatively low variation than the longer one. The horizontal and vertical component's precision level was estimated to less than one and two meters. This is likely due to the existence of obstructions along the route.

The presented results were obtained during the fieldwork tests. Hence, the factors affecting the GNSS signal propagation (i.e., the multipath and atmospheric bias) are challenging to be identified. We suggest that future studies should be carried out

in controlled environments and situations. For example, collecting data in different types of obstruction and time.

REFERENCES

- Alcay, S. and Turgut, M. (2017) Performance Evaluation of Real-Time Precise Point Positioning Method. *IOP Conference Series: Earth and Environmental Science*, 95(3). <https://doi.org/10.1088/1755-1315/95/3/032023>
- BIG (Badan Informasi Geospasial). (2013). *Sistem Referensi Geospasial Indonesia 2013, Peraturan Kepala BIG No. 15*. Badan Informasi Geospasial
- Bramanto, B., Gumilar, I. and Kuntjoro, W. (2015) RT-PPP: Concept and Performance in Indonesia Region. *FIT ISI 2015*. Batu: ISI. <https://isi.or.id/papermakalah/>
- Bramanto, B., Gumilar, I., Abidin, H. Z., Prijatna, K., and Adi, F.S. (2017) Assessment of the BeiDou Data Quality and the Positioning Performance: A Perspective from Bandung, Indonesia. *Journal of Aeronautics, Astronautics and Aviation, Series A*, 49(2), 191-204. <https://doi.org/10.6125/17-0202-929>
- CO (Cabinet Office). (2018) *Quasi-Zenith Satellite System Performance Standard (PS-QZSS-001)*. <https://qzss.go.jp/en/technical/download/pdf/ps-is-qzss/ps-qzss-001.pdf>
- El-Hattab, A. (2014) Assessment of PPP for establishment of CORS network for municipal surveying in Middle East. *Survey Review*, 46(335), 97-103. <https://doi.org/10.1179/1752270613Y.0000000064>
- El-Mowafy, A. (2018) Predicting orbit and clock corrections during their outage in real-time positioning using GPS, GLONASS and QZSS for natural hazard warning systems. *Journal of Applied Geodesy*, 13(2), 1-11. <https://doi.org/10.1515/jag-2018-0043>
- Ge, M., Gendt, G., Rothacher, M., Shi, C., and Liu, J. (2008) Resolution of GPS carrier-phase ambiguities in precise point positioning (PPP) with daily observations. *Journal of Geodesy*, 82(7), 389-399. <https://doi.org/10.1007/s00190-007-0187-4>
- Gumilar, I., Bramanto B., Pamungkas, A.I., Abidin, H.Z. and Adi, F. S. (2017) Contribution of BeiDou Positioning System for Accuracy Improvement: A Perspective from Bandung, Indonesia. *Journal of Aeronautics, Astronautics and Aviation, Series A*, 49(3), 171-184. <https://doi.org/10.6125/17-0202-930>
- Gumilar, I., Bramanto, B., Kuntjoro, W., Abidin, H.Z. and Trihantoro, N.F. (2018) Contribution of BeiDou satellite system for long baseline GNSS measurement in Indonesia. *IOP Conference Series: Earth and Environmental Science*, 149(1):012070. <https://doi.org/10.1088/1755-1315/149/1/012070>
- Gumilar, I., Ananta, R.Y., Bramanto, B., Abidin, H.Z., Surono and Kishimoto, N. (2021) Initial performance assessment of GNSS augmentation system using Quasi-Zenith Satellite System for Real-Time Precise Positioning method in Indonesia. *IOP Conference Series: Earth and Environmental Science*, 767(1): 012021. <https://doi.org/10.1088/1755-1315/767/1/012021>
- Hofmann-Wellenhof, B., Lichtenegger, H. and Waskle, E. (2007) *GNSS – Global Navigation Satellite Systems*. Wien: Springer-Verlag

- JAXA (Japan Aerospace Exploration). (2017) *Quasi-Zenith Satellite System (QZSS) First Quasi-Zenith Satellite System 'MICHIBIKI'*. https://global.jaxa.jp/countdown/f18/pdf/presskit_michibiki_e.pdf
- Kobayashi, K. (2020) *QZSS-PPP Service MADOCA/CLAS*. Tokyo: GNSS Lab. ICG Programme on GNSS Applications: Training on GNSS
- Kouba, J. and Héroux, P. (2001) Precise point positioning using IGS orbit and clock products. *GPS Solution*, 5(2), 12-28. <https://doi.org/10.1007/PL00012883>
- Krasuski, K. (2015) Utilization GPS/QZSS Data for Determination of User's Position. *Pomiary Automatyka Robotyka*, 19(2), 71-75
- Moschas, F., Avallone, A., Saltogianni, V. and Stiros, S. (2014) Strong motion displacement waveforms using 10-Hz precise point positioning GPS: An assessment based on free oscillation experiments. *Earthquake Engineering and Structural Dynamics*, 43(12), 1853-1866. <https://doi.org/10.1002/eqe.2426>
- Murai, Y. (2014) Project Overview: Quasi-Zenith Satellite System. *Proceedings of the 27th International Technical Meeting of the Satellite Division of the Institute of Navigation ION GNSS+ 2014 (Florida)*, 2974-3008
- Namie, H. and Kubo, N. (2021) Performance Evaluation of Centimeter-Level Augmentation Positioning L6-CLAS/MADOCA at the beginning of official operation of QZSS. *IEEJ Journal of Industry Applications*, 10(1), 27-35. <https://doi.org/10.1541/ieejia.20001080>
- Ramachandran, D., Din, A., Ibrahim, S. and Omar, A. (2019) Real-Time Precise Point Positioning (RT-PPP) for Positioning and Mapping. In B. Pradhan, *Lecture Notes in Civil Engineering* Vol 9 (pp. 891-913). Singapore: Springer
- Thombre, S., Bhuiyan, M.Z.H., Söderholm, S., Kirkko-Jaakkola, M., Ruotsalainen, L. and Kuusniemi, H. (2016) A Software Multi-GNSS Receiver Implementation for the Indian Regional Navigation Satellite System, *IETE Journal of Research*, 62(2), 246-256, <https://doi.org/10.1080/03772063.2015.1093968>
- Takahashi, H. (2004) Japanese Regional Navigation Satellite System "The JRANS Concept". *Journal of Global Positioning System*, 3(1-2), 259-264
- Takasu, T., Ebinuma, T. and Yasuda, A. (2009) Effect of Quasi Zenith Satellite (QZS) on GPS Positioning. http://gpspp.sakura.ne.jp/paper2005/isgps_2009_qzs_8_.pdf
- Teunissen, P. and Montenbruck, O. (2017) *Handbook of Global Navigation Satellite System*. Springer
- Wu, F., Kubo, N. and Yasuda, A. (2004) Performance Evaluation of GPS Augmentation Using Quasi-Zenith Satellite System. *IEEE Transactions on Aerospace and Electronic Systems*, 40(4), 1249-1260. <https://doi.org/10.1109/TAES.2004.1386878>
- Zhang, Y., Wu, F. and Yasuda, A. (2007) Impact of Integrated GPS and The Quasi-Zenith Satellite System in the East Asian Region. *Transactions of the Japan Society for Aeronautical and Space Sciences*, 50(168), 105-112. <https://doi.org/10.2322/tjsass.50.105>
- Zhu, S., Yue, D., He, L., Liu, Z. and Chen, J. (2020) Comprehensive Analysis of Compatibility between QZSS and GPS in Asia-Pacific Region: Signal Quality, RTK and PPP. *Advances in Space Research*, 66(2), 395-411. <https://doi.org/10.1016/j.asr.2020.04.003>